Comparison of numerical and analytical approaches for simulating purely sinusoidal voltammetry

Henry O. Lloyd-Laney,[†] Martin J. Robinson,[†] Alison Parkin,[*,‡] and David J. Gavaghan[*,†]

[†]*Department of Computer Science, University of Oxford, Wolfson Building, Parks Road, Oxford, OX1 3QD United Kingdom*

[‡]*Department of Chemistry, University of York, Heslington, York, YO10 5DD, United Kingdom*

E-mail: alison.parkin@york.ac.uk; david.gavaghan@dtc.ox.ac.uk

Abstract

In this paper we present a comparison of two mathematical techniques for simulating the behaviour of a surface-confined single-electron redox process when interrogated with a large amplitude sine-wave. The two simulation methods are an analytical approximation proposed by Bell and co-authors, and a numerical solution that we have previously used to analyse such single-electron processes. We show that the techniques are in good agreement, allowing for the limitations imposed by the construction of the analytical model. We also compare two different parameter inference approaches proposed for the respective simulation techniques.

Introduction

In a recent paper,[1] we showed the advantages of using a large amplitude sinusoidal potential input, a technique we termed Purely Sinusoidal Voltammetry (PSV), to interrogate the redox-reactions of surface-confined molecules. The principal advantage of this technique is the ability it gives to numerically simulate a complete experiment faster than other similar voltammetric techniques, while offering a reasonable degree of sensitivity to important electrochemical reaction parameters. The act of simulation requires solving a system of differential equations to obtain the total current as a function of Faradaic, background current and experimental input parameters; the forward problem. In our previous work, we have used numerical methods when solving the forward problem, in part because the same simulation approach can be used for multiple potential input waveforms for a given mechanism. There is a large pool of literature that uses numerical approaches in the solving of the forward and inverse problems, reviewed by Gavaghan[2] and Bieniasz.[3] A unified mathematical approach is rarely possible for analytical solutions to the forward problem, which often require an array of complex mathematics and a variety of constraints to achieve an expression for either the total current or some feature derived thereof, such as in the work of Bazant.[4,5] However, there are certainly advantages to using a tractable analytical solution, such as not having to account for numerical error, and reductions in the computational burden. Prior to our work showing that it was possible to infer parameters from experimental PSV data using the numerical approach,[1] Bell et al. published an analytical approximation (referred to for convenience as "the analytical method") for the total current arising from a surface confined PSV experiment (which they termed "large-amplitude sinusoidal voltammetry").[6] In this paper, we have reproduced some of the work of Bell et al., demonstrating that the solution obtained by the numerical and analytical approaches is equivalent. This validates the accuracy of our numerical approach, as two independent mathematical methods for modelling the same system yielding the same solution is a sufficient criterion for confidence in both. In addition, Bell and co-authors suggested several approaches for inferring chemical

reaction parameter values based on features of the current arising from a large-amplitude sinusoidal voltammetry experiment. We evaluate the performance of one of these approaches, and investigate the accuracy of the recovery in the presence of increasing values of noise. We compare the inference results to our own parameter inference method, using Markov-chain Monte Carlo methods to infer parameter distributions from the total current. Our results indicate that, although this parameter inference approach based on analysis of distinct current features (as opposed to the total current) is grounded in very solid mathematics, it is highly sensitive to noise. We discuss plans to expand this analysis to other heuristic analyses in voltammetry.

Derivation of simulation models

Both the analytical method proposed by Bell,[6] and our numerical approach start from the same point, and model the current arising from a surface-confined species undergoing a single-electron redox reaction, described by the following chemical equation

$$\mathrm{Ox} \underset{k_{ox}}{\overset{k_{red}}{\rightleftharpoons}} Red + \mathrm{e}^{-}.$$

The current as a function of time $\tilde{i}(\tilde{t})$ is dependent on the rate of change of the surface concentration of the oxidised species $\tilde{\theta}_{ox}$

$$\tilde{i}(\tilde{t}) = FA\frac{d\tilde{\theta}_{ox}}{d\tilde{t}}, \tag{1}$$

where the rate of change of $\tilde{\theta}_{ox}$ is calculated from mass-action kinetics

$$\frac{d\tilde{\theta}_{ox}}{d\tilde{t}} = \tilde{k}_{ox}(\tilde{t})\tilde{\theta}_{red} - \tilde{k}_{red}(\tilde{t})\tilde{\theta}_{ox}. \tag{2}$$

We use the Butler-Volmer equations to represent $\tilde{k}_{ox}$ and $\tilde{k}_{red}$, using the rate constant

$\tilde{k}^0$, and the symmetry factor α

$$\tilde{k}_{ox}(\tilde{t}) = \tilde{k}^0 \exp\big((1-\alpha)(\tilde{E}(\tilde{t}) - \tilde{E}^{0'})\big), \tag{3}$$

and

$$\tilde{k}_{red}(\tilde{t}) = \tilde{k}^0 \exp\big(-\alpha(\tilde{E}(\tilde{t}) - \tilde{E}^{0'})\big), \tag{4}$$

where $\tilde{E}(\tilde{t})$ is defined as

$$\tilde{E}(\tilde{t}) = \tilde{E}_{in} + \Delta\tilde{E}\sin(\tilde{\omega}\tilde{t}), \tag{5}$$

where $\tilde{E}_{in}$ is the average input voltage, or $\frac{E_{start}+E_{reverse}}{2}$ as long as the signal is periodic. Equation 2 can be non-dimensionalised in multiple different ways, depending on what parameter(s) is/are chosen to non-dimensionalise the time constant. Both the numerical and analytical methods share the following approach

$$\tilde{E}^0 = \frac{RT}{F}E^0, \quad \tilde{E}(\tilde{t}) = \frac{RT}{F}E(t), \quad \tilde{\theta} = \theta\tilde{\theta}_{tot},$$

for the analytical case, time is non-dimensionalised using the rate constant k^0 such that

$$\tilde{t} = \frac{t}{\tilde{k}^0}, \quad \tilde{i}(\tilde{t}) = FA\tilde{k}^0\tilde{\theta}_{tot}i(t), \quad \omega = \frac{\tilde{\omega}}{\tilde{k}^0},$$

and for the numerical case, we non-dimensionlise time using the period of an oscillation of the potential input, v

$$\tilde{t} = \frac{t}{v}, \quad \tilde{i}(\tilde{t}) = FAv\tilde{\theta}_{tot}i(t), \quad \omega = \frac{\tilde{\omega}}{v},$$

At this point, the method for obtaining the current for the two methods diverge — we detail the approaches for the analytical method in the supplementary information, and our numerical methodology can be found in previous papers.[1] The key result from the derivation for the analytical case is that the error in the expression is dependent on the inverse of the

dimensionless input frequency ω^{-1}.

Comparing the analytical and numerical models of PSV

Table 1: Simulation parameters used to generate analytical and numerical simulations as compared in figure 2. Parameters marked with an asterisk were not modelled in the analytical approximation, and set to zero for the numerical solution. The values of the parameters were largely taken from Bell et al.[6]

Parameter	Symbol (Unit)	Value
Start potential	$\tilde{E}_{start}$ (V)	-0.25
Reverse potential	$\tilde{E}_{reverse}$ (V)	0.25
Midpoint potential	$\tilde{E}^0$ (V)	0.1
Rate constant	$\tilde{k}_0(s^{-1})$	Variable
Uncompensated resistance	$\tilde{R}_u$ (Ω)	0*
Linear double-layer capacitance	$\tilde{C}_{dl}$ (F)	0*
Surface coverage	$\tilde{\theta}_{tot}$ (mol cm^{-2})	1.0E-11
Symmetry factor	α	0.55
Potential frequency	$\tilde{\omega}$ (Hz)	Variable
Potential amplitude	$\Delta\tilde{E}$ (V)	0.25
Area	A (cm^2)	0.03

In order to check the validity of the numerical approach, we compare the predicted dimensional current generated using the numerical and analytical solutions, using the simulation parameters in table 1. We show the impact of increasing frequency on the analytical and numerical currents in figure 1. We see that higher input frequencies lead to increasing agreement between the numerical and analytical solutions, as predicted by the error term discussed in the derivation section. The fact that there is good agreement between the analytical and numerical approaches implies we can have confidence in our numerical approach.

The comparison in figure 1 is undertaken more comprehensively in figure 2, where the relative error was calculated using the expression in equation 6, where RMSE is the root mean square error, and i_a and i_n are the analytical and numerical currents respectively. The error

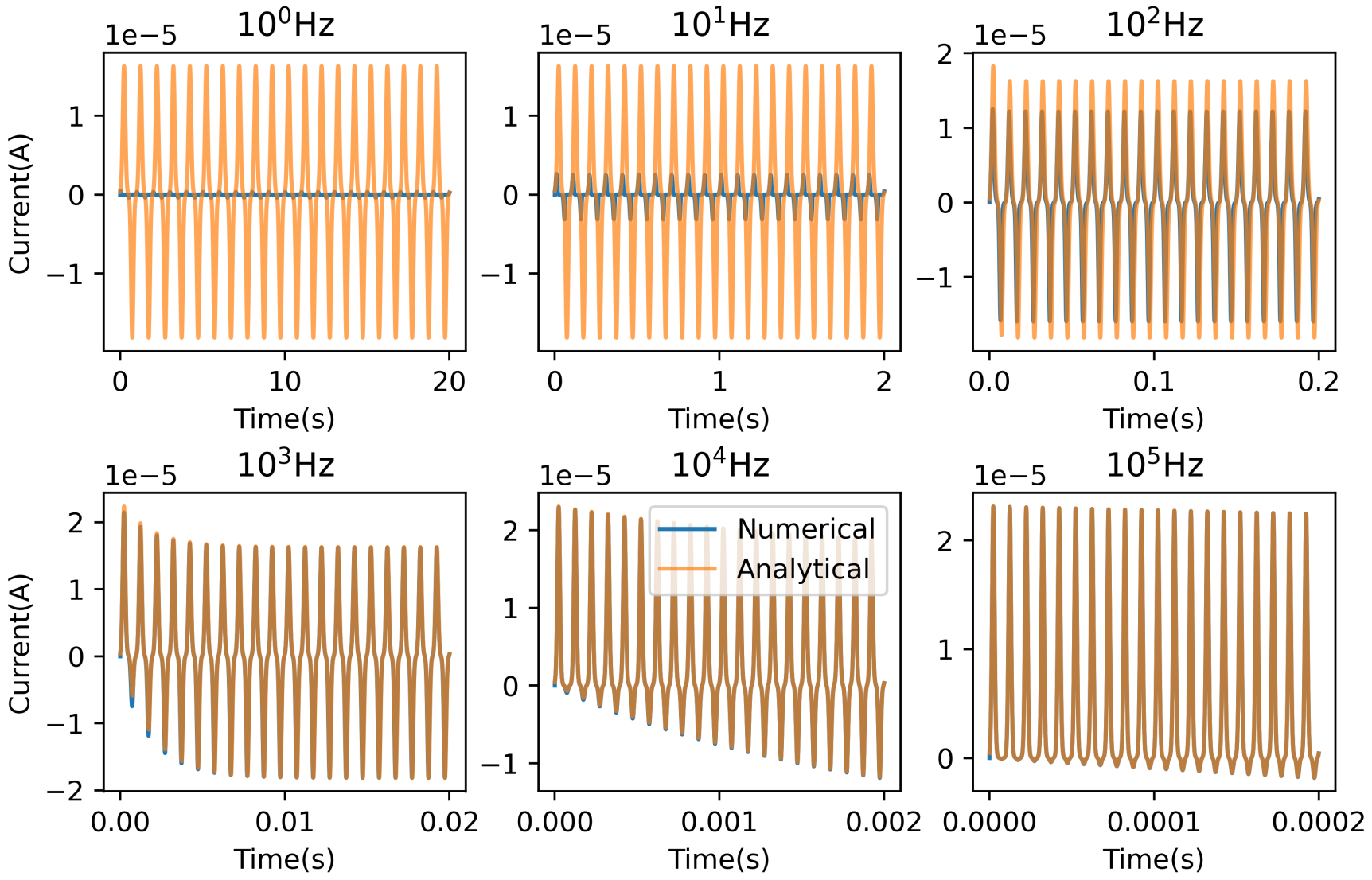

Figure 1: Current simulated using analytical and numerical methods against time. The value of the input frequency is shown in the title of each plot, and all other paramaters are as in table 1, with $\tilde{k}^0$ set to 10.

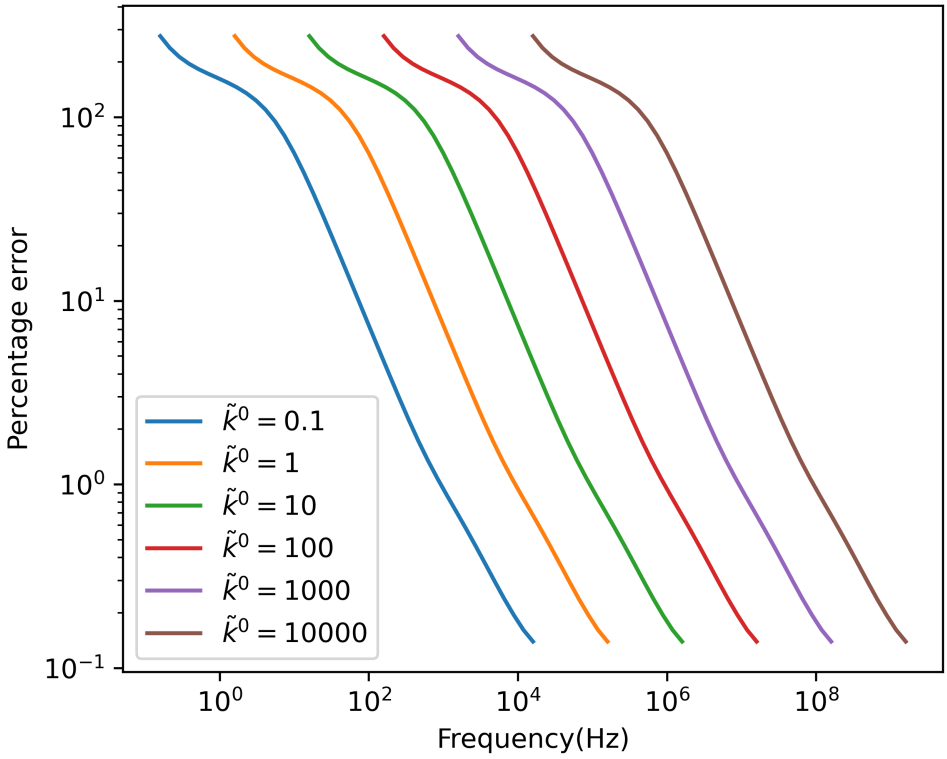

Figure 2: Percentage error of the analytical and numerical currents as function of the kinetic parameter k^0 and the input frequency. The kinetic value $\tilde{k}^0$ in units of s^{-1} is shown in the legend, with the rest of the simulation parameters reported in table 1.

is expressed as a percentage in figure 2.

$$\text{Relative difference} = \frac{\text{RMSE}(i_a, i_n)}{\bar{i}_n} \tag{6}$$

As expected, the accuracy of the analytical expression is dependent on the size of the input frequency, because of the assumption that took us from equation S8 to equation S9 in the SI. Additionally, because of the choice of non-dimensionalisation, we can predict the order of magnitude of the error. Because the analytical approximation error is proportional to the inverse of the frequency $O(\omega^{-1})$, this can be represented as $O(X\%)$, where X is the ratio $\frac{\tilde{k}^0}{\tilde{\omega}}$. As noted by Bell and coauthors,[6] for the error to be $O(1\%)$, $\tilde{\omega}$ must be 100 times the magnitude of $\tilde{k}^0$. However, we observe that in figure 2, 1% error is only observed with

an input frequency that is four magnitudes larger than the kinetic parameter. This may be because of our choice of error measure (as the true value of the current is not known), and it should be noted that a similar result is observed when calculating the current using a numerical simulation of equation S2 in the SI. From these comparisons it is apparent that the frequency needs to be very large to obtain an analytical current simulation that agrees with the numerical simulations, in some cases larger than is experimentally realisable. While there are some advantages to solving the forwards problem this way, in particular computational speed, the issue remains that the choice of frequency affects the amount of information contained within the experimental current for a given system. If we use the analytical approach, then we are obligated to use a frequency that minimises the approximation error. In addition, the analytical approximation does not account for the impact of non-linear double layer capacitance and uncompensated resistance (R_u), both of which we have found to be key parameters when attempting to fit to experimental PSV data. As our numerical model incorporates both of these parameters, they were set to zero when generating the numerical solution, as inclusion of these effects would unnecessarily complicate the analysis presented here.

Inferring parameters from synthetic noisy data

Bell et al. also reported a way to use the analytical approximation discussed above to infer two key parameters, the reversal potential E^0 and the kinetic parameter k_0. This requires undertaking two PSV experiments on the same system with different potential input amplitudes. The inference approach requires taking the absolute magnitudes of the harmonics of the current for each experiment, which is combined along with several other parameters including the potential amplitude ΔE, the symmetry factor α and the average input potential E_in to provide an expression for the reversible potential E^0. The value of E^0 can then be used to calculate the value the kinetic parameter.[6] This method work perfectly

in the noiseless regime, but as we show in figure 3, the harmonic amplitude ratio is sensitive to the addition of noise. Current data was simulated using the analytical method described above, using the parameters in table 2 for 300 potential oscillations, and normal, independent and identically distributed (I.I.D.) random variables were added at each time point, with a mean of zero and a standard deviation which was a percentage of the maximum value of the current. We attempted to infer the $\tilde{E}^0$ parameter using the ratio of the harmonic amplitudes from two "noisy" simulations obtained using two different ΔE values, as described in.[6] This process was repeated 1000 times for each noise value, and we plot the calculated $\tilde{E}^0$ values as a histogram on the left-hand plot in figure 3. To compare this to the numerical approach, we simulated current using the numerical method, using the same parameters and also for 300 oscillations, and added noise using the same approach described above. We then ran an adaptive Metropolis-Hastings algorithm to infer parameter distributions from this data, the results of which are shown on the right in figure 3.

Table 2: Simulation parameters used to generate analytical and numerical simulations from which the $\tilde{E}^0$ distributions in 3 were inferred. Parameters marked with an asterisk were not modelled in the analytical approximation, and set to zero for the numerical solution. Two input potential amplitudes are used for the analytical inference method. For the numerical method only the lower values was used. The values of the parameters were chosen to closely mimic the inference examples given in the paper by Bell et. al

Parameter	Symbol (Unit)	Value
Start potential	$\tilde{E}_{start}$ (V)	-0.077/0.128
Reverse potential	$\tilde{E}_{reverse}$ (V)	0.077/-0.128
Midpoint potential	$\tilde{E}^0$ (V)	0.0257
Rate constant	$\tilde{k}_0(s^{-1})$	1
Uncompensated resistance	$\tilde{R}_u$ (Ω)	0*
Linear double-layer capacitance	$\tilde{C}_{dl}$ (F)	0*
Surface coverage	$\tilde{\theta}_{tot}$ (mol cm^{-2})	1.0E-11
Symmetry factor	α	0.55
Potential frequency	$\tilde{\omega}$ (Hz)	50
Potential amplitude	$\Delta\tilde{E}$ (V)	0.077/0.128
Area	A (cm^2)	0.03

We see from this figure that the error in the inferred $\tilde{E}^0$ value increases with increasing

Table 3: Means and standard deviations (in brackets) of the histograms of inferred $\tilde{E}^0$ values shown in figure 3 for analytical and numerical inference approaches.

Noise %	Analytical inferred $\tilde{E}^0$ (V)	Numerical inferred $\tilde{E}^0$ (V)
5.0%	0.0375 (0.0208)	0.0255 (0.000109)
4.0%	0.0351 (0.0158)	0.0258 (8.388E-05)
3.0%	0.0331 (0.0132)	0.0257 (6.572E-05)
2.0%	0.0306 (0.00955)	0.0258 (4.322E-05)
1.0%	0.0285 (0.00653)	0.0257 (2.246e-05)

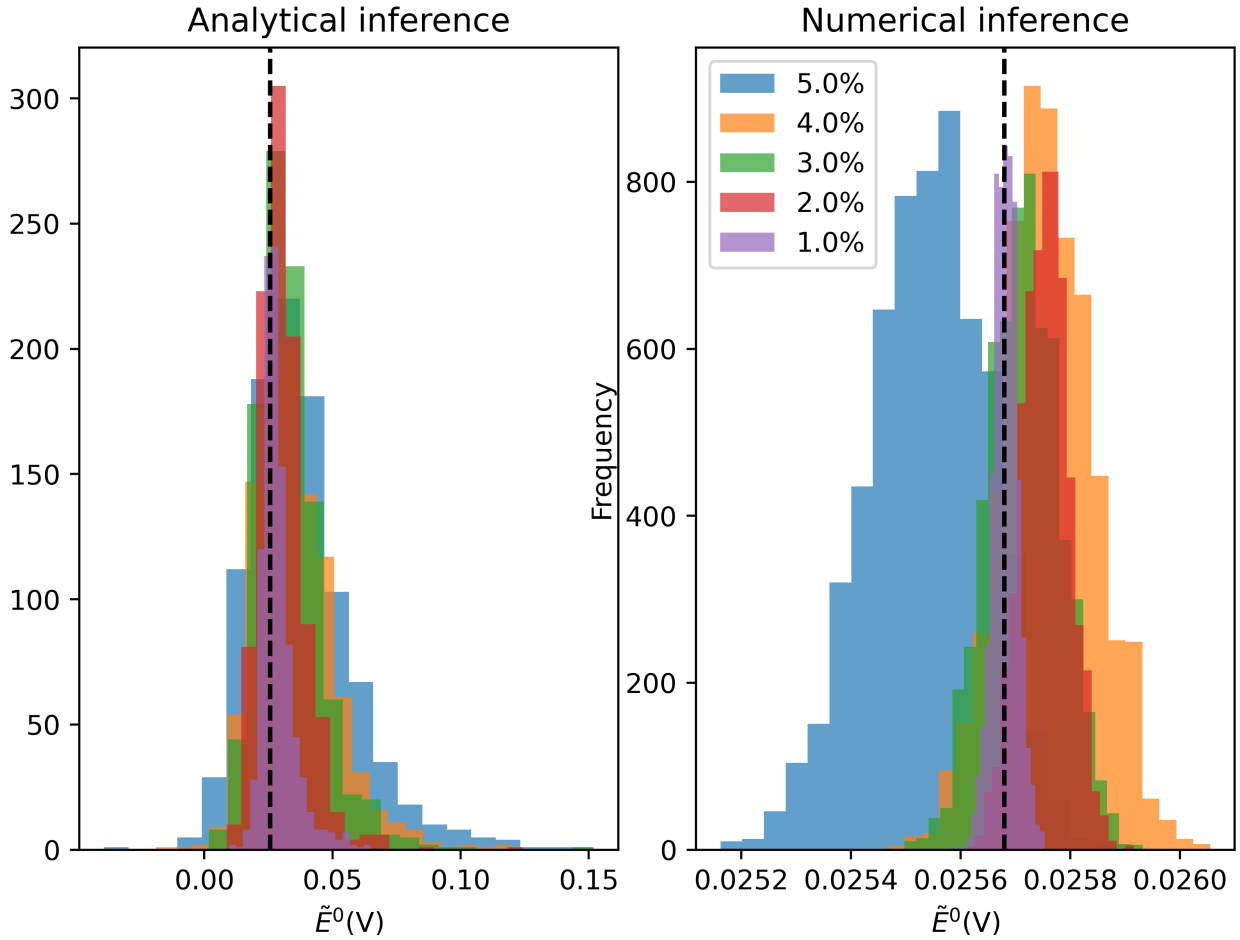

Figure 3: Left: Histogram of $\tilde{E}^0$ values obtained from synthetic noisy PSV data, generated using the analytical method described above. I.I.D. normal noise was added at every time-point, with 0 mean and an standard deviation that was a percentage of the maximum value of the analytical current, indicated in the legend. The process of adding noise and calculating the $\tilde{E}^0$value was repeated 1000 times for each percentage, and the average inferred $\tilde{E}^0$value was plotted. Right: Histogram of inferred $\tilde{E}^0$ values generated by pooling the last 1000 samples from three MCMC chains run for 10000 iterations. In both cases the true simulation $\tilde{E}^0$ value is indicated by a black line.

noise for both cases. In table 3 we see that the numerical approach yields estimates of the $\tilde{E}^0$ that are closer to the true value and with a standard deviation that is approximately 2 orders of magnitude lower. It should be noted that for the analytical inference method, any errors in the inferred $\tilde{E}^0$ value will be propagated to the estimate of the $\tilde{k}_0$ value as well. In terms of inferring data about actual experimental systems, we have observed that the level of noise in data obtained from a surface-confined ferrocene coated electrode is typically around 0.5% of maximum current — which means that the analytical inference approach could potentially be used to corroborate the results of our numerical inference process in low noise systems. However, in our experience, the un-modelled effects of R_u and C_{dl} both have significant effects on harmonic amplitude, which will skew the results of this process.[6]

Conclusions

In this paper we have demonstrated very good agreement in the limit of high frequency between our previously presented numerical solution of a surface-linked, single-electron redox process interrogated using PSV, and the analytical model of the same system presented by Bell et al. We have shown that there is a good agreement between two mathematical models for the same experiment, confirming the legitimacy of the numerical approach. We have also determined that, while the analytical approach is very accurate in the regime under which it was derived (high input frequency and low noise), its use as a predictive tool appears to decrease as we move towards real-world conditions, such as the presence of noise and limitations of equipment. We believe that the method comparison detailed here, of taking heuristic methods derived under favourable assumptions, and observing the robustness of the predictions to increasing noise when the true answers are known, is a valuable way of benchmarking the utility of these methods. This may be useful for theoretical scientists who hope to see more widespread adoption of their ideas amongst experimentalists, as it allows for a demonstration of how the technique performs under likely experimental conditions

where the presence of noise makes the inference problem more challenging.

References

(1) Lloyd-Laney, H.; Robinson, M.; Hewson, A. R.; Firth, J.; Zhang, J.; Bond, A.; Parkin, A.; Gavaghan, D.; Yates, N.; Elton, D. Using Purely Sinusoidal Voltammetry for Rapid Parameterization of Surface-Confined Electrochemistry. **2020**,

(2) Gavaghan, D. J.; Cooper, J.; Daly, A. C.; Gill, C.; Gillow, K.; Robinson, M.; Simonov, A. N.; Zhang, J.; Bond, A. M. Use of Bayesian inference for parameter recovery in DC and AC Voltammetry. *ChemElectroChem* **2018**, *5*, 917–935.

(3) Bieniasz, L.; Speiser, B. Use of sensitivity analysis methods in the modelling of electrochemical transients: Part 3. Statistical error/uncertainty propagation in simulation and in nonlinear least-squares parameter estimation. *Journal of Electroanalytical Chemistry* **1998**, *458*, 209–229.

(4) Bazant, M. Z.; Chu, K. T.; Bayly, B. J. Current-voltage relations for electrochemical thin films. *SIAM journal on applied mathematics* **2005**, *65*, 1463–1484.

(5) Bazant, M. Z.; Thornton, K.; Ajdari, A. Diffuse-charge dynamics in electrochemical systems. *Physical review E* **2004**, *70*, 021506.

(6) Bell, C. G.; Anastassiou, C. A.; O'Hare, D.; Parker, K. H.; Siggers, J. H. Theory of high frequency, large-amplitude sinusoidal voltammetry for ideal surface-confined redox systems. *Electrochimica acta* **2011**, *56*, 7569–7579.